Proceedings of the Institute of Acoustics

SCALING OFFSHORE PILE DRIVING NOISE: APPLICATION TO FREQUENCY WEIGHTED SOUND LEVELS

J von Pein DHI Wasy GmbH, Hamburg, Germany
M Ram DHI Wasy GmbH, Hamburg, Germany
F Thomsen DHI A/S, Hørsholm, Denmark

1 INTRODUCTION

The biological impact of pile driving noise during the installation of offshore wind turbines is one of the key issues for the environmental management of marine renewable energies in Europe and beyond. Pile driving leads to relatively high impulsive noise emissions into the water, which can be a potential threat to marine life. Therefore, the accurate prediction of the emitted acoustical energy is a prerequisite for any biological risk assessment of offshore pile driving noise. Usually, numerical or empirical models based on measurements are used to assess the sound exposure level (SEL) that is emitted into the water column during piling[1,2]. Both approaches have the disadvantage that only few institutions and experts have access to them. As an alternative that is available for all regulators as well as the industry, scaling laws have been developed that are applied to existing data to estimate the emitted sound during offshore pile driving. The scaling laws define the dependence of the broadband SEL on the strike energy E, pile diameter d, water depth h_w, and ram weight m_r for scenarios without noise mitigation, see von Pein *et al.*[3].

To asses the species specific impact of the emitted sound levels, weighting functions are applied to account for different hearing characteristics[4]. The ongoing development of scaling laws for the one-third octave band spectrum of the SEL allows for the evaluation of scaling laws for frequency weighted SELs[5].

The study aims to investigate whether scaling laws derived for weighted SELs have a similar accuracy to those derived for the unweighted SEL[3] and thus potentially provide another tool freely available to regulators and industrial professionals.

The scaling laws for weighted SELs are derived by applying the identified frequency dependent scaling laws to the average of measured spectra and thus deriving the weighted SEL as a function of pile diameter and water depth.

In the following, the frequency dependent scaling laws are applied to weighted spectra to derive a first estimate of the influence of the water depth and pile diameter on the NOAA-LF-, NOAA-PW-, and NOAA-HF-weighted SEL[4], which are referred to as LF-, PW-, and HF-weighted SEL. The respective weighing functions are shown in Fig. 1.

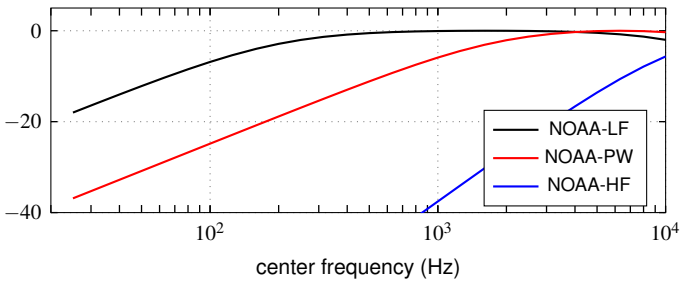

Figure 1: The considered NOAA weighting functions.

2 FREQUENCY DEPENDENT SCALING LAWS

The results of the model runs presented in von Pein *et al.*[3] combined with additional model runs are evaluated to derive the dependence of the one-third octave band spectrum of the SEL on the pile diameter and the water depth.

It is important to note that the scaling laws derived in the following are based on generalizations, assumptions and numerical model runs that come along with uncertainties. Furthermore, not all effects that may play a role at the considered frequency range are covered within the numerical model and are therefore also not covered within the scaling laws.

The influence of the strike energy is assumed to be frequency independent and is scaled with

$$\Delta\mathrm{SEL}_E = 10\log_{10}\left(\frac{E_i}{E_0}\right). \tag{1}$$

The influence of the hammer type is usually taken into account in detailed numerical models by computing the interaction between hammer and pile. The hammer and pile geometries have a considerable influence on the specific frequency bands, which is hard to generalize. Therefore, the ram weight is also scaled without a frequency dependence by the broadband scaling law

$$\Delta\mathrm{SEL}_{m_r} = -10\log_{10}\left(\frac{m_{r,i}}{m_{r,0}}\right). \tag{2}$$

2.1 Pile diameter

The influence of the pile diameter on the one-third octave band spectrum of the SEL is displayed in Fig. 2. Therein the differences between the computed SEL with a diameter of 2 m and results derived with diameters up to 15 m are displayed. It can clearly be seen that the increase at low frequencies is much higher compared to the increase at higher frequencies. This is linked to the higher increase in the radiation efficiency at low frequencies. In order to derive a frequency dependent scaling law the equation

$$\Delta\mathrm{SEL}_d(f) = k_d(f)\log_{10}\left(\frac{d_i}{d_0}\right) \tag{3}$$

is fitted to every individual considered one-third octave band. The resulting frequency dependent coefficient $k_d(f)$ is displayed within the right plot of Fig. 2.

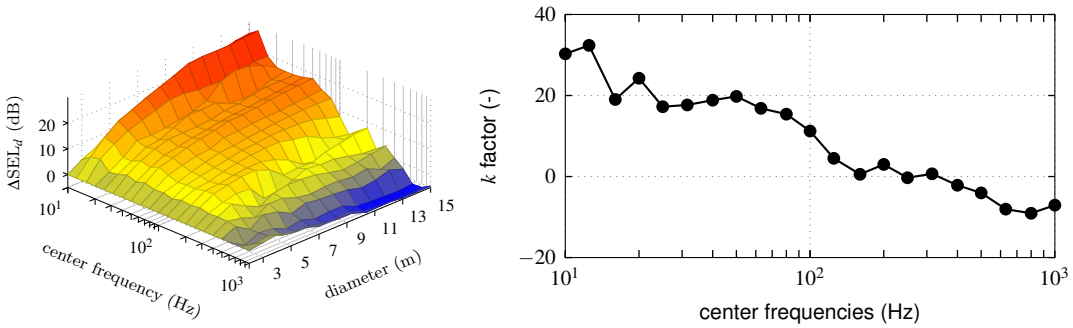

Figure 2: The differences between the computed SEL at a range of 20 m over the center frequencies and the considered diameters (left) and the frequency dependent scaling factors $k_d(f)$ fitted for every individual frequency band (right).

2.2 Water depth

The influence of the water depth on the one-third octave band spectrum can be separated into four different main effects.

The cutoff effect describes the influence of the water depth on the lowest frequency that is able to propagate. Since the affected frequency range is well above the cutoff frequency, this effect is not considered in the following.

The water depth in combination with the pile geometry (diameter, length, wall thickness), soil type, and the penetration depth define the modal shapes of the pile. The influence of distinct modes is mainly at frequencies up to 100 Hz.

The actual interaction behavior of pile and water depends on several factors such as the pile geometry and soil. An attempt is made to generalize these. However, its influence on the weighted levels is rather small due to the affected frequencies.

Frequencies of up to 200 Hz showed in the results that the influence of the water depth can be scaled

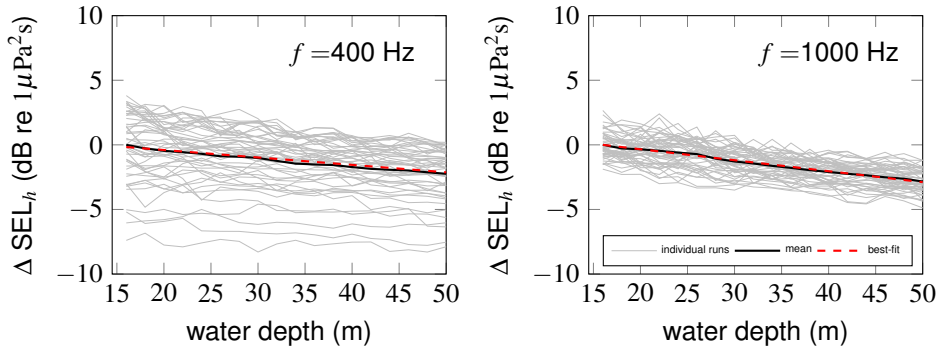

Figure 3: The dependence of the SEL on the water depth evaluated at 20 m derived with 50 different geometry combinations.

with the damping term of the Damped Cylindrical Spreading model[6] as presented in[3].

As shown in Fig. 3, frequencies above 200 Hz show a linear decaying trend in the SEL with increasing water depth. This linear decay becomes more distinct with increasing frequency.

2.3 Application to measurements

In the following the sources of the publicly available measurement data sets are described. Measurement data averaged from positions in three different directions at the range of 750 m is available from the Borkum Riffgrund 1 (BR1) wind farm[7]. Measurement results from Prinses Amaliawindpark (PA)[8] and of two different piles from the Gemini (GE)[9] wind farm from the Dutch part of the North Sea are considered. The data set from the USA derived at a test monopile within the Coastal Virginia Offshore Wind (CV) project[10] is also considered. The major parameters of the mentioned sites are listed in Table 1. The considered measured spectra of the sites are displayed in Fig. 4.

Table 1: Details of the piling configurations used for the validation.

wind farm	strike energy (kJ)	pile diameter (m)	water depth (m)	ram weight (t)	hammer type
PA	800	4	22	95	MHU 1900S
BR1	800	5.9	27	100	Hydrohammer S-2000
GE2	894	6.6	30	100	Hydrohammer S-2000
GE1	1486	7	34	100	Hydrohammer S-2000
CV	687	7.8	24	150	Hydrohammer S-3000

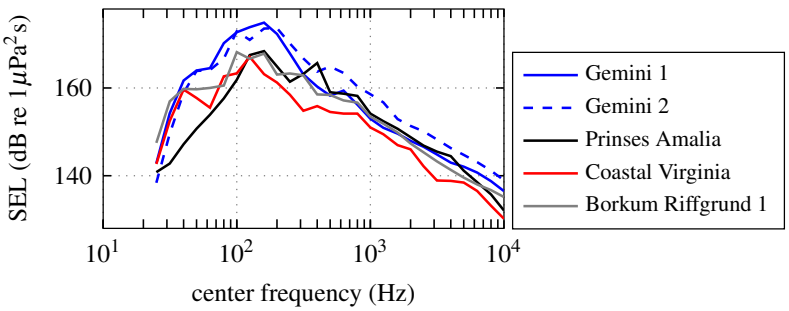

Figure 4: The unscaled measured spectra of several different wind farms.

The available spectra are scaled to the arbitrarily chosen parameters $E_i = 2000$ kJ, $d_i = 8$ m, $h_w = 40$ m and $m_{r,i} = 200$ t. The scaled results are displayed in Fig. 5 together with the respective mean. The shape of the mean is very similar to spectra provided by Bellman *et al.*[2]. The mean of the scaled results is the base line for the derivation of the dependencies of the weighted SELs on the pile diameter and the water depth conducted in the following sections.

3 SCALING LAWS FOR WEIGHTED SEL

In the following, the logarithmic mean of the scaled spectra from Fig. 5 is scaled with the frequency dependent scaling laws for the pile diameter and the water depth. Finally, the considered weighting is applied and the weighted SEL evaluated. Since the measurements have been derived at a range of

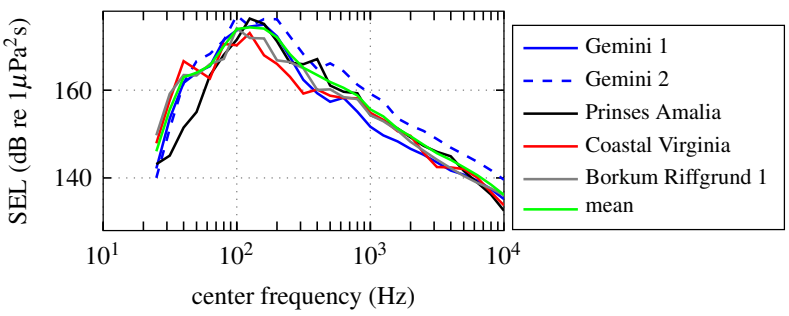

Figure 5: The scaled spectra of several different wind farms scaled to the parameters $E_i = 2000$ ***kJ,*** $d_i = 8$ ***m,*** $h_w = 40$ ***m and*** $m_{r,i} = 200$ ***t.***

750 m it is important to note that the scaling laws are valid for this range. At ranges further away, the site specific propagation effects will dominate the acoustical outcome.

3.1 Influence of the Pile Diameter

The dependence of the three weighted SEL on the pile diameter are displayed in Fig. 6. Therein, a logarithmic trend can be seen for the LF SEL, a linear trend for the PW weighting, and a negligible influence can be seen for the HF weighting. Best-fit approximations lead to the scaling laws of $\Delta\mathrm{SEL}_{\mathrm{LF},d} = 12.5\log_{10}(d_i/d_0)$ and $\Delta\mathrm{SEL}_{\mathrm{PW},d} = 0.4(d_i - d_0)$.

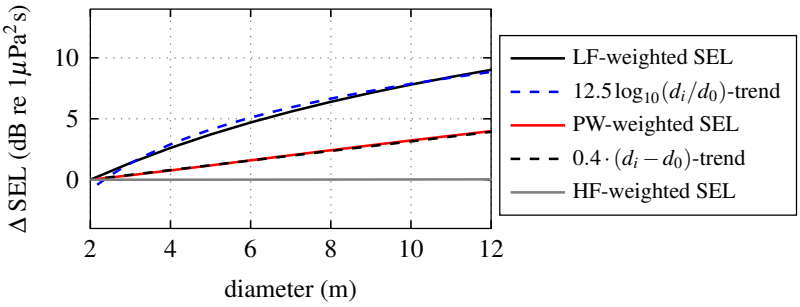

Figure 6: The dependence of the weighted SEL on the pile diameter.

3.2 Influence of the Water Depth

The evaluated influence of the water depth on the weighted SEL are displayed in Fig. 7. Therein, the LF-SEL dependence on the water depth is dominated by the change in the propagation effect that is scaled with the DCS model for the unweighted SEL and can be approximated with $\Delta\mathrm{SEL}_{LF,h_w} = 1.7\log_{10}(h_i/h_0)$ for the LF-weighted SEL. In the case of PW and HF-weighting the dependence of the SEL on the water depth is negative. These can be summarized with best-fit approximations of $\Delta\mathrm{SEL}_{PW,h_w} = -0.04(h_i - h_0)$ for PW and $\Delta\mathrm{SEL}_{HF,h_w} = -0.1(h_i - h_0)$ for HF-weighting.

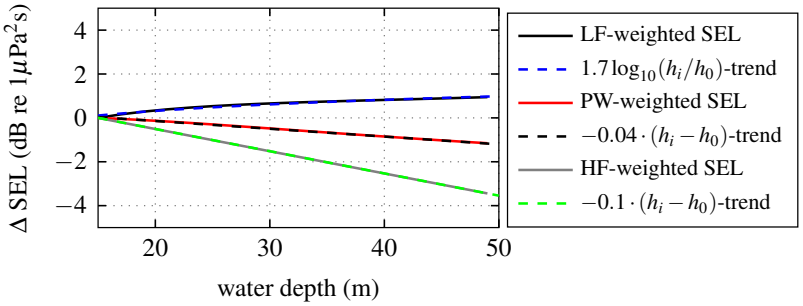

Figure 7: The dependence of the weighted SEL on the water depth.

3.3 Comparison to measurements

In the following the weighted SELs are scaled to an artificial scenario with the parameters $E_i = 2000$ kJ, $d_i = 8$ m, $h_w = 40$ m and $m_{r,i} = 200$ t. Within Fig. 8 the LF-, PW-, and HF-weighted SEL scaled with the application of the obtained scaling laws are displayed over the water depth (left column) and over the pile diameter (right column). Within every plot the results obtained by applying strike energy and ram weight scaling are compared to the results obtained by additional pile diameter scaling (left column) and additional water depth scaling (right column). The trend that has not been applied to the scenarios is also shown.

Since only five data points are available and they cover only a small parameter space, the comparison of the derived trends to the measurements can not be regarded to be a sufficient validation. However, the difference between the upper and lower bounds are about 5.9 dB for the LF-weighted SEL, 5.2 dB for the PW-weighted SEL, and 4.9 dB for the HF-weighted SEL, which is a similar range as shown by von Pein *et al.*[3] in the validation of the scaling laws for the broadband SEL. Another indicator for the derived scaling laws pointing into the right direction is the reduction of the standard deviation from the initial value of the measured weighted SEL to the E-, E-m_r-, E-m_r-d, and E-m_r-d-h_w-scaled results. In the case of LF-weighted SELs the standard deviation of the measurements is 3.9 dB. The application of E-scaling leads to a reduced value of 2.8 dB, which is even further reduced to 2.4 dB by E-m_r-scaling. Applying all four scaling terms reduces the standard deviation of the scaled measurements to 2.2 dB. The same evaluation leads for the PW-weighted SEL to standard deviations of 3.2, 2.4, 2.1, and 2.2 dB and for the HF-weighted SEL to 2.7, 2.1, 1.9, and 2.0 dB. For all weighted SEL the E-m_r-scaling leads to a lower standard deviation. The application of E-m_r-d-h_w-scaling is only for the LF-SEL able to even further reduce the standard deviation.

4 CONCLUSION AND OUTLOOK

It has been shown that there is a way to derive scaling laws for weighted SELs and that the derived dependencies of the weighted SELs on the pile diameter and water depth are less severe compared to the trends derived for the unweighted SEL presented in a previous paper. This indicates that the unweighted SEL increases significantly more with increasing diameter and increasing water depth than the weighted SELs. The comparison to measurements show that the application of the frequency independent E-m_r-scaling reduces the standard deviation for all considered weighted SEL. The additional application of d and h_w-scaling has only a minor effect on the standard deviation. It leads to a reduction for the LF-weighted SEL and to a minor increase for the PW- and HF-weighted SEL.

The range between upper and lower bound of the scaled measurements are in a similar range as for the unweighted SEL. The presented scaling laws for weighted SELs provide a straightforward means of estimating the influence of strike energy, pile diameter, ram weight, and water depth on weighted SELs.

This paper represents a promising starting point for the development of scaling laws for frequency-weighted SELs. However, to enable a more profound validation of the frequency-dependent scaling laws and scaling laws for weighted SEL, further non-disclosed measurement data with a greater variety of the parameters such as pile diameter and water depth is necessary.

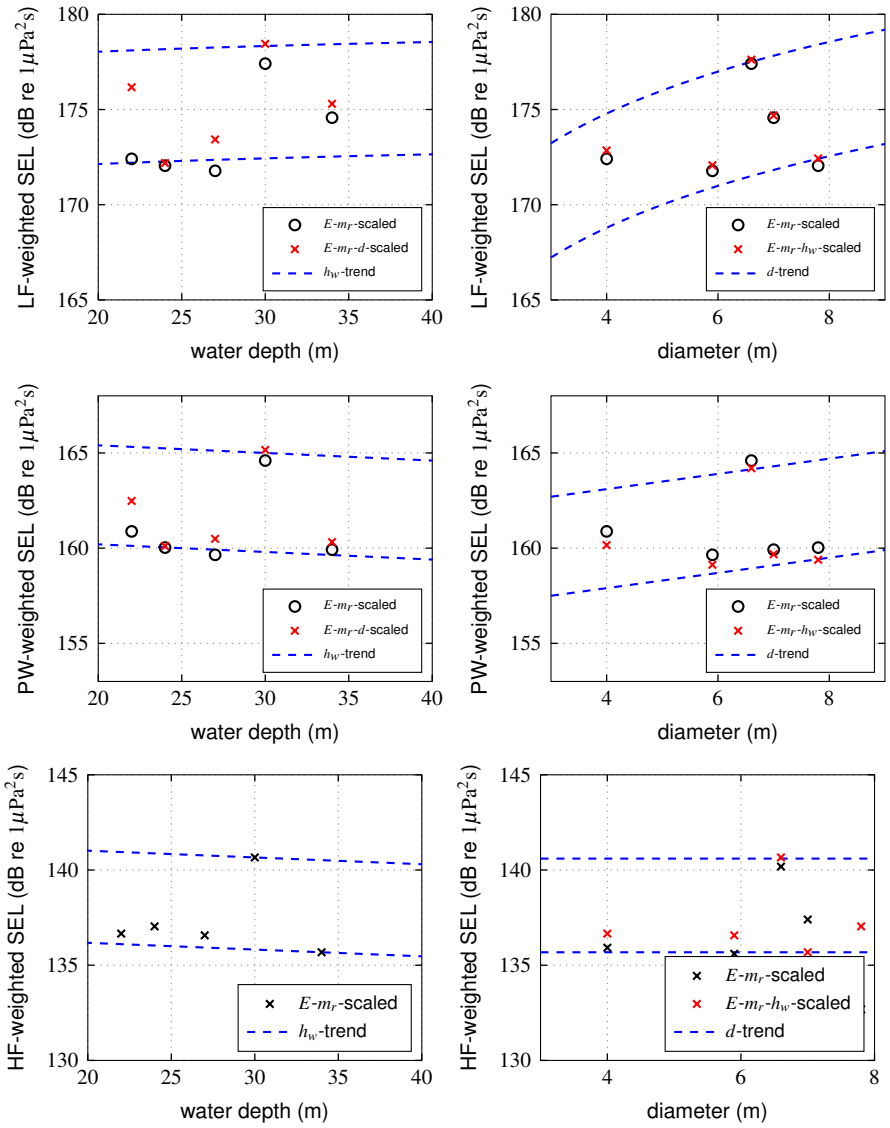

Figure 8: The scaled weighted SEL over the water depth (left column) and over the pile diameter (right column).

REFERENCES

1. J. von Pein, S. Lippert and O. von Estorff, ”Validation of a finite element modelling approach for mitigated and unmitigated pile driving noise prognosis”, *The Journal of the Acoustical Society of America* **149**(3), 1737-1748 (2021)
2. M. A. Bellmann, A. May, T. Wendt, S. Gerlach and P. Remmers, ”Underwater noise during the impulse pile-driving procedure: Influencing factors on pile-driving noise and technical possibilities to comply with noise mitigation values”, (2020).
3. J. von Pein, T. Lippert, S. Lippert and O. von Estorff, ”Scaling laws for unmitigated pile driving: Dependence of underwater noise on strike energy, pile diameter, ram weight, and water depth”, *Applied Acoustics* **198**, (2022).
4. National Marine Fisheries Service: Summary of Endangered Species Act acoustic thresholds (marine mammals, fishes and sea turtles) (2023).
5. J. von Pein, T. Lippert, S. Lippert and O. von Estorff, ”Frequency Dependent Scaling Laws for Offshore Pile Driving Noise”, Presentation at the Underwater Acoustics Conference and Exhibition in Kalamata, Greece (2023).
6. T. Lippert, M. A. Ainslie and O. von Estorff, ”Pile driving acoustics made simple: Damped cylindrical spreading model”, *The Journal of the Acoustical Society of America* **143**(1), 310-317 (2018).
7. M. A. Bellmann, S. Gündert and P. Remmers, ”Offshore Messkampagne 3 (OMK3) für das Projekt BORA im Offshore-Windpark Borkum Riffgrund 01 (Offshore measurement campaign 3 (OMK3) for the BORA project at the wind farm Borkum Riffgrund 01)”, (2015).
8. C. de Jong and M. Ainslie, ”Underwater sound due to piling activities for Prinses Amaliawindpark” (2012).
9. P. Remmers and M. A. Bellmann, ”Ecological monitoring of underwater noise during piling at Offshore Wind Farm Gemini” (2015).
10. J. Brinkkemper, ”Coastal Virginia Offshore Wind - Noise monitoring during monopile installation A01 and A02”, (2020).